(DOI: will be inserted by hand later)

Triggered massive-star formation on the borders of Galactic H II regions

I. A search for 'collect and collapse' candidates

L. Deharveng, A. Zavagno, and J. Caplan

Laboratoire d'Astrophysique de Marseille, 2 Place Le Verrier, 13248 Marseille Cedex 4, France e-mail: lise.deharveng@oamp.fr

Received 03/09/2004; accepted 30/11/2004

Abstract. Young massive stars or clusters are often observed at the peripheries of H II regions. What triggers star formation at such locations? Among the scenarios that have been proposed, the 'collect and collapse' process is particularly attractive because it permits the formation of massive objects via the fragmentation of the dense shocked layer of neutral gas surrounding the expanding ionized zone. However, until our recent article on Sh 104, it had not been convincingly demonstrated that this process actually takes place. In the present paper we present our selection of seventeen candidate regions for this process; all show high-luminosity near-IR clusters and/or mid-IR point sources at their peripheries. The reality of a 'collect and collapse' origin of these presumably second-generation stars and clusters will be discussed in forthcoming papers, using new near-IR and millimetre observations.

Key words. Stars: formation – Stars: early-type – ISM: H II regions

1. Introduction

Statistical studies have shown that the presence of an H II region contiguous to a molecular cloud has two effects on star formation in the cloud: an increased rate of formation in general, and increased formation of massive objects in particular. For example, Dobashi et al. (2001) investigated the luminosity of protostars in molecular clouds, as a function of the cloud mass, in a sample of 499 clouds taken from the literature; 243 of these clouds turned out to be associated with protostar candidates selected from the IRAS Point Source Catalog. They showed that the protostars in clouds adjacent to H II regions are more luminous than those in the clouds away from H II regions. Finding that there are well-defined upper and lower protostar luminosity limits, they proposed a very simple model in which the protostar luminosity is controlled by the mass of the parental cloud and by an external pressure exerted upon the cloud surface. The lower and upper limits of the luminosity distribution correspond to external pressures of zero and $\sim 10^{5.5} k \text{ K cm}^{-3}$, where k is the Boltzmann constant. This latter figure is a reasonable value for the pressure of the ionized gas in a classical H п region.

Detailed studies of large star-forming regions also show that the presence of an H $\scriptstyle\rm II$ region favours star formation, especially of massive objects. Karr and Martin (2003), in their multi-wavelength study of the W5 H $\scriptstyle\rm II$ region, found that the

number of star-formation events per unit CO covering area is 4.8 times higher within the influence zone of the H π region than outside. Also, in their study of the Vela molecular ridge, Yamaguchi et al. (1999) found that the average luminosities of IRAS sources in clouds associated with H π regions and in clouds far from H π regions are 780 L_{\odot} and 63 L_{\odot} respectively.

Several processes, presented in Sect. 2, have been proposed for triggering star formation at the peripheries of H II regions (Elmegreen 1998). We are particularly interested in the 'collect and collapse' process because it permits the formation of massive objects – stars or clusters. This process, first proposed by Elmegreen & Lada (1977) has not, until now, been convincingly confirmed. The aim of the present paper is to propose a list of carefully selected candidate regions which are likely to be examples of this process at work. We present our selection criteria in Sect. 3, we discuss the general mid-IR features of the selected regions in Sect. 4, and we briefly comment on the individual regions in Sect. 5. We have observed most of these regions in the near-IR and a few at millimetre wavelengths; these studies will be presented in separate papers (one of which – Deharveng et al. 2003b – has already been published), in which we will investigate the reality of the collect and collapse process. Finally, we present a discussion and conclusion in Sect. 6.

2. Possible processes triggering star formation at the periphery of an $H_{\rm II}$ region

Consider a massive first-generation star that forms an H π region. Due to the high pressure of the warm ionized gas relative to that of the surrounding cold neutral material, the H π region expands; its expansion velocity is of the order of 11 km s⁻¹ just after the ionization of the gas and the formation of the initial Strömgren sphere, and it decreases with time (Dyson & Williams 1997).

During the expansion of the H II region various events may occur.

- 1. The H_{II} region may expand into an inhomogeneous medium containing pre-existing molecular clumps. The pressure exerted by the ionized gas on the surface of a clump can lead to its implosion, and to the formation of a 'cometary globule' surrounded by dense ionized gas forming a 'bright rim' (see Bertoldi 1989, Bertholdi & McKee 1990, and Lefloch & Lazareff 1994 for a simulation of the evolution of such a globule). During the short collapse phase, a shock front progresses into the clump, leading to the formation of a dense core. This collapse is followed by a transient phase of re-expansion and then by a quasi-stationary cometary phase. During this last phase the cometary globule has a dense head and a tail extending away from the ionizing source; the globule slowly evaporates as the dense ionized gas flows away from it. All the signs of recent star formation are observed in the direction of cometary globules: IRAS sources with protostellarobject colours, MSX point sources, near-IR reddened objects, CO outflows, Herbig-Haro objects, H α emission stars, etc. (e.g. Lefloch et al. 1997, Sugitani et al. 1989, Ogura et al. 2001 and Thompson et al. 2004). However, no model explains where star formation takes place (in the core, or at its periphery) or when (during the maximum compression phase, or earlier).
- 2. The ionization front of the Hπ region is supersonic and is preceded by a shock front in the neutral gas. With time, neutral material accumulates between these two fronts. This compressed, shocked material may become dynamically unstable on a *short* internal-crossing timescale. This configuration was simulated by García-Segura & Franco (1996): the shell of neutral material fragments, creating clumps which are afterward slowly eroded by the ionization front, leading to the formation of cometary globules and bright rims. The difference with the previous process is that the dense clumps do not pre-exist, but are formed as the result of instabilities in the collected layer.
- 3. The compressed shocked layer may become gravitationally unstable along its surface, on a *long* timescale. This is the 'collect and collapse' model, first proposed by Elmegreen & Lada (1977). This process allows the formation of massive fragments. For example, according to Whitworth et al. (1994), the compressed layer around the H II region formed by an O7 star, evolving in a medium of 10³ cm⁻³, with a sound speed of 0.5 km s⁻¹ in the layer, will become unstable after about 3 Myr; about seven fragments will form, each with a mass ~ 600 M_☉. These fragments are dense

and they will very quickly fragment in turn, leading to the formation of a cluster of coeval stars.

If the collected layer is not destroyed quickly by dynamical instabilities, a large quantity of material accumulates within it. This is the reason why its fragmentation (as a consequence of gravitational instabilities) produces *massive* fragments – massive enough to form massive stars and/or clusters. Also, these fragments are *regularly spaced around the H n region*.

- 4. The H π region may form and evolve within a supersonic turbulent molecular medium (Elmegreen et al. 1995). Clumps are formed by turbulence compression in the gas. As the ionization front and its associated shock move into the cloud, these clumps are collected into the compressed layer; they merge into a few massive postshock cores. These may collapse gravitationally, forming a cluster. In this case, the dense cores would be *randomly* distributed around the H π region.
- 5. A completely different process is proposed by Fukuda & Hanawa (2000) who consider the interaction between an H π region and a nearby filamentary molecular cloud. As the H π region expands, the cloud is pinched and separated into two parts. A gravitational instability induces the formation of two cores along the filament axis. As this process is recursive, core formation and, hence, possibly star formation propagates along the filament axis.

3. Selection of candidate H II regions

To show that the collect and collapse mechanism is at work in a given star-formation zone, the following predictions must be verified by observations:

- A neutral compressed layer should surround the H II region. Being quite dense, the material must be molecular; and being a thin spherical shell, the layer should appear as a ring when projected on the plane of the sky. Hence the compressed layer should be observed as a ring of molecular line emission at millimetre wavelengths. Furthermore, since the layer contains dust, it should also be observed as a ring of mid-IR and millimetre emissions.
- The fragments should be dense, massive and *regularly* spaced along the surface of the shell.
- Second generation stars or clusters, formed in the expanding layer, will have retained the velocity of the material in which they formed. Thus they should be observed in the direction of the layer, or slightly in front of it (on the neutral side) if the layer is slowing down.

The presence of several fragments *regularly* spaced along the compressed layer is a strong argument in favour of the collect and collapse process, as it allows us to reject processes involving pre-existing molecular clumps, or clumps formed by random turbulence.

None of the examples proposed by Elmegreen (1998) to illustrate the collect and collapse model are completely convincing, as the morphologies of these regions are complex, so that it is impossible to verify if the above conditions are satisfied. If we want to prove that the collect and collapse process works,

we need to study objects with a very simple morphology, where a clearly defined ionization front separates the ionized gas from the dense neutral surrounding medium. Therefore we have used the following criteria to select such candidate regions:

- A nearly spherical H II region around an exciting star or cluster.
- A dust-emission ring surrounding the ionized gas. We have used the MSX Band A survey at 8.3 μm (see Sect. 4) to search for such rings. As explained in Sect. 4, this emission comes mainly from large molecules polycyclic aromatic hydrocarbons (PAHs) situated in the photo-dissociation region surrounding the ionized gas. The presence of this dust ring indicates that dense neutral gas surrounds the H II region.
- An MSX point source in the direction of the dust ring. (We call a 'point source' any source listed in the MSX Point Source Catalog (Egan et al. 1999, 2003), even though some are in fact resolved by MSX.) We expect these MSX point sources to trace small dust grains that are locally heated by an embedded cluster or by a massive object.
 - The dense clumps (and subsequently the clusters) resulting from the fragmentation of the compressed layer can be located anywhere in the spherical shell. We realize that by rejecting those regions with MSX point sources which happen to project *inside* the dust ring, we are eliminating many legitimate cases where sources happen to be located more nearly in front of or behind the H II region. If 'nearly' means, say, within 45° of the line of sight, then 70.7% of the shell projects on the ring. If there are three point sources, the chances are only 0.707³, or 35%, that none falls inside the ring. This is a high price to pay, but it nearly guarantees that a clump or cluster really lies in the vicinity of the compressed layer.
- Red stars or clusters associated with the MSX point sources. We have used the 2MASS Survey to search for these objects.

For northern hemisphere regions, we have used the NVSS radio continuum survey at 1.4 GHz (Condon et al. 1998), to see if ultracompact (UC) radio sources are present in the direction of the MSX point sources.

Table 1 lists the selected sources. Column 1 gives the name of the H II region surrounded by the MSX Band A emission ring, and columns 2 and 3 the (approximate) coordinates of its centre. Columns 4 and 5 give the coordinates of the MSX point source(s) observed in the direction of the ring (sometimes several are observed; we are interested here by the brighter ones). Column 6 gives the corresponding IRAS source, and column 7 the distance of the region. Column 8 indicates the observations which we have subsequently made of these regions.

The H II region Sh 104 is the prototype of such objects (see its description in Sect. 5). In the first of our planned detailed studies, already published (Deharveng et al. 2003b), we have shown that this region is a good illustration of the collect and collapse process. Our present aim is to find other, similar regions susceptible to confirm this process and provide observations to further constrain the model.

4. Mid-IR emission of the selected sources

The mid-IR emission from Galactic H_{II} regions depends on their evolutionary status (UC or more evolved) and has been studied by many authors, both spectroscopically and with imaging, using ground-based and space facilities. The main results of these studies can be summarized as follows: the spectra of UC H II regions show a continuum emission increasing with wavelength, and strong silicate absorption features centred at 9.7 and $18 \mu m$ (cf. Faison et al. 1998). More evolved H II regions also show a continuum emission increasing with wavelength, but superimposed on the continuum are mid-IR bands, the unidentified infrared bands (UIBs), centred at 6.2, 7.7, 8.6, 11.3 and 12.7 μ m. These emission bands have been attributed to large molecules such as polycyclic aromatic hydrocarbons, PAHs (Léger & Puget 1984). Inside the ionized gas the dominant emission is the continuum emission from small grains, stronger for earlier-type exciting stars; beyond the ionization front, the emission is predominantly from large molecules such as PAHs (cf. Zavagno & Ducci 2001). Small grains can survive in strong UV fields, while large molecules cannot (cf. Crété et al. 1999, Peeters et al. 2002). Atomic fine-structure lines and hydrogen recombination lines are also present in the spectra of H II regions (see Peeters et al. 2002 for UC H II regions).

The mid-IR spectra of Herbig Ae/Be stars (intermediate mass pre-main-sequence stars) show large star-to-star differences. Most present a continuum emission increasing with wavelength; some exhibit a strong silicate emission near $10~\mu m$, others PAH emission bands (Bouwman et al. 2001, Meeus et al. 2001).

Mid-IR emission associated with H II regions has been studied by Crowther & Conti (2003 – for UC regions) and by Ghosh & Ojah (2002) and Conti & Crowther (2003 – for more evolved ones) using the Midcourse Space eXperiment (MSX) with the on-board instrument SPIRIT III (Price et al. 2001). This experiment has surveyed the entire Galactic plane (|b| < 5 deg) in four mid-IR bands – A, C, D and E – centred at 8.3, 12.13, 14.65 and 21.34 μ m respectively, with an angular resolution of about 18". The MSX Band A includes the dominant UIBs at 7.7 and 8.6 μ m. This band also includes the silicate feature at 9.7 μ m. The MSX Band C includes the UIBs at 11.3 and 12.7 μ m, as well as continuum emission. In UC H II regions, the continuum dominates and increases continuously from Band C to Band E.

We have used the MSX Bands A and E in order to characterize the mid-IR emission of the extended sources in Table 1. Fig. 1 presents colour composite images of four regions – Sh 104, RCW 79, RCW 82 and RCW 120. The Band A emission is displayed in turquoise and the Band E emission in red. The Band A emission, dominated by the UIBs, forms a ring around the H II region. Band E, dominated by the continuum emission from small grains, peaks *inside* the turquoise ring, in the direction of the ionized gas. These images show the importance of studying objects with simple morphologies, in which emissions of various origin are clearly separated in the plane of the sky. These regions unambiquiously demonstrate that: i) the UIB carriers do not survive in the ionized gas, but are present in the photo-dissociation region where they are excited by the UV radiation leaking from the H II region; ii) the small grains

Table 1. Selected regions.

	<u> </u>	177 .		1.637		ID A C	D: .	<u> </u>
		ral H II region			nt source	IRAS	Distance	Comments
1	Sh 104	$20^{\rm h}17^{\rm m}42.^{\rm s}0$	+36°45′25′′	20 ^h 17 ^m 56. ^s 6	+36°45′39′′	20160+3636	4.0	1, 3, 4
2	X	20 20 48.05	+39 34 43	20 20 46.1	+39 35 14		?	1
3	Y	1 01 09.5	+62 54 08	1 01 08.4	+62 54 44	00580+6238	1.9	1
4	Sh 212	4 40 38.9	+50 27 44	4 40 27.2	+50 28 29	04366+5022	7.1	1
5	Sh 217	4 58 45.4	+47 59 58	4 58 30.3	+47 58 33a	04547+4753	5.0	3, 4
6	Sh 219	4 56 10.5	+47 23 36	4 56 03.3	+47 22 57	04523+4718	5.0	3
7	Z near Sh 230	5 23 09.95	+33 58 13	5 23 03.7	+33 58 31	05197+3355	1.8 - 3.2	1, 4
8	Sh 241	6 03 58.6	+30 15 25	6 03 54.0	+30 14 49	06006+3015	4.7	1, 4
9	Sh 259	6 11 27.7	+17 26 17	6 11 23.7	+17 26 29	06084+1727	8.3	1, 4
10	RCW 34	8 56 28.0	$-43\ 06\ 00$	8 56 27.7	$-43\ 05\ 47$	08546-4254	3.1	2
11	RCW 40	9 02 22.0	$-48\ 41\ 55$	9 02 07.1	$-48\ 43\ 27$		2.4	5
12	RCW 40			9 02 28.5	-48 39 14	09007-4827		5
13	Dutra 45	10 19 51.4	-58 04 09	10 20 15.7	-58 03 57	10184-5748	4.5	2
14	Dutra 46	10 29 31.0	$-57\ 26\ 45$	10 29 32.4	$-57\ 26\ 36$	10276-5711	6.2	2
15	RCW 71	12 50 21.1	-61 34 58	12 50 25.0	-61 35 34	12474-6119	2.1	5
16	RCW 79	13 40 17.0	$-61\ 44\ 00$	13 40 53.1	-61 45 51	13374-6130	4.0	2, 5
17	RCW 82	13 59 29.0	$-61\ 23\ 40$	13 59 57.1	$-61\ 24\ 37$	13563-6109	2.9	2
18	RCW 82			13 59 03.6	-61 22 17	13555-6107		
19	RCW 120	17 12 23.1	-38 27 43	17 12 40.9	-38 27 08	17092-3823	1.3	5

^a Not in the Point Source Catalog; we have measured its position on the MSX Band A frame.

Comments

- 1. JHK observations at CFHT.
- 2. JHK_S observations with the NTT telescope at ESO.
- 3. molecular line emission observations at IRAM.
- 4. 1.2 mm continuum emission at IRAM.
- 5. 1.2 mm continuum emission with the SEST at ESO.

responsible for the mid-IR emission are not destroyed in the ionized gas, and compete with the gas to absorb the Lyman continuum photons emitted by the exciting stars.

We have also used the MSX fluxes (given in Table 2) of the point source(s) observed towards the dust ring, to tentatively determine their nature, either UC H II regions or intermediate mass Herbig Ae/Be stars. As shown previously, each type of object possesses a characteristic mid-IR spectrum depending on its nature and/or evolutionary status. Mid-IR colour-colour diagrams can therefore be used to determine the nature of the observed point sources. Egan et al. (2001) and Lumsden et al. (2002) have combined near-IR and mid-IR colour-colour diagrams to identify different kinds of MSX point sources. They have shown that all the young sources (Herbig Ae/Be stars, massive young stellar objects and UC H II regions) are well separated from the bulk of normal stars, a consequence of the large extinction due to the fact that the young objects are embedded in optically-thick dust clouds. These authors have also shown that the UC H II regions and the Herbig Ae/Be stars occupy different positions in the F_{14}/F_8 versus F_{21}/F_{14} and the F_{14}/F_{12} versus F_{21}/F_8 diagrams (Fig. 2). Their explanation is that the Herbig Ae/Be stars are the least embedded of the young sources, which is reflected in their having bluer colours than the other objects. An alternative explanation is that, due to the fact that the spectra near 10 µm of some Herbig Ae/Be stars are dominated by the silicate emission feature (Meeus et al. 2001), their Band A emission is enhanced.

UC H II regions have been clearly detected as radio continuum sources in the direction of the MSX point sources associated with Sh 104, Sh 217 and RCW 79. However, few of the other sources in Table 1 have been observed in the radio continuum with an angular resolution high enough to allow the detection of a UC H II region – if any – at the border of the central H II region. Therefore we have used the mid-IR colours of the MSX point sources to get an idea about their nature – do they contain stars massive enough to ionize the gas, or intermediate-mass stars? Fig. 2 shows the position of the MSX point sources of Table 2 in Lumsden et al.'s (2002) colour-colour diagrams. The two diagrams give consistent information: some of the MSX point sources – those observed at the borders of Sh 212, Sh 259, RCW 34, Dutra 45 and RCW 82 (18) – are probably associated with UC H II regions.

We can also use the far-IR luminosities of the MSX point sources, given in Table 2, to get additional information about the presence of massive stars (assuming that the radiation of the young objects is reprocessed by dust, and emerges in the far IR). The far-IR flux can be obtained from the observed IRAS fluxes (Table 2) using the relation (Emerson 1988 cited by Lumsden et al. 2002)

 $F_{\rm FIR} = (20.6F_{12} + 7.54F_{25} + 4.58F_{60} + 1.76F_{100})~{\rm W~m}^{-2}$. The far-IR luminosities are obtained from these fluxes using the distances given in Table 1. Using the effective temperatures of main-sequence stars and their radii, according to Smith et al. (2002), the luminosity of a B1.5V star is $17800~L_{\odot}$. No figures are given by these authors for a B2V star. We will

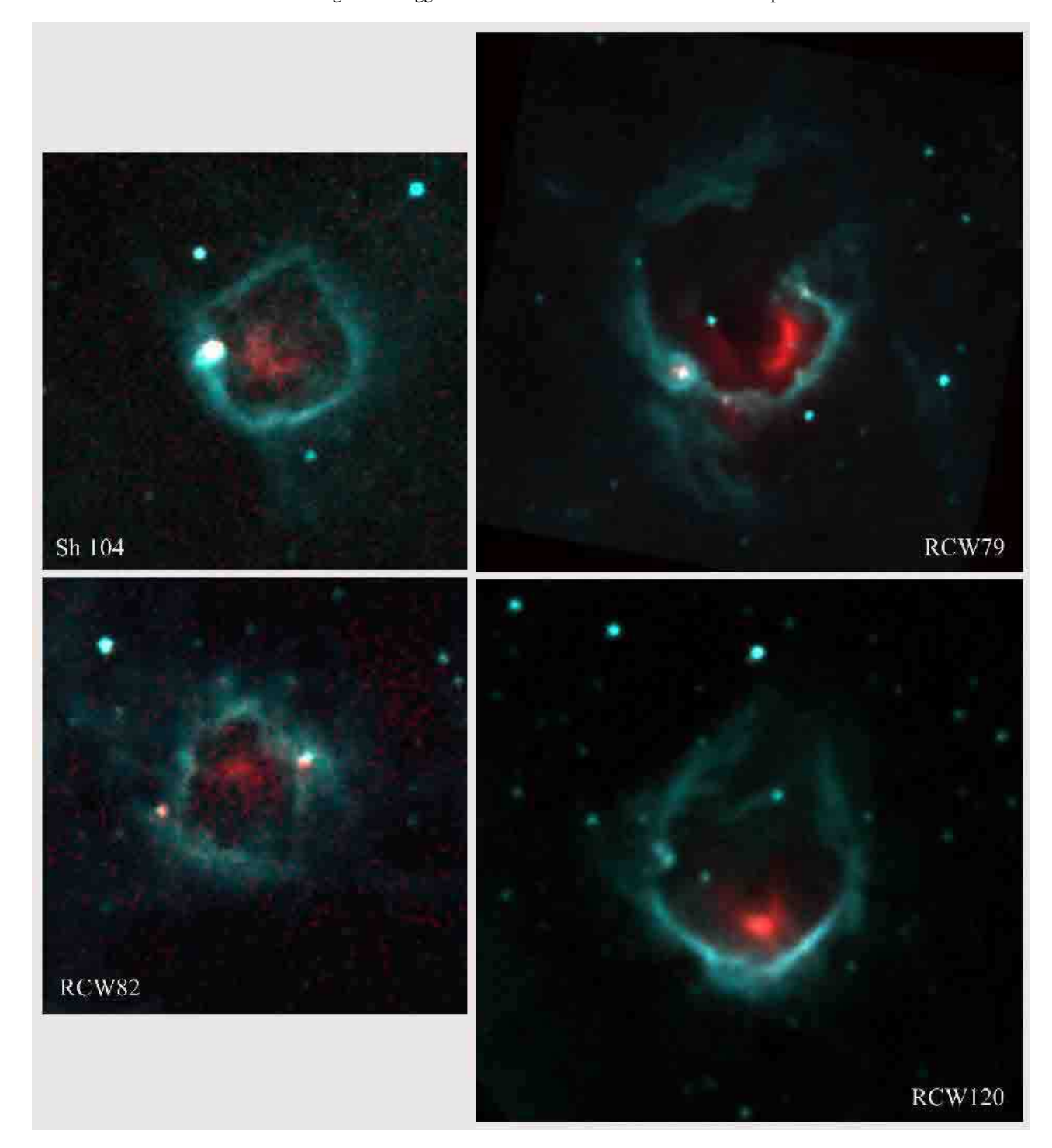


Fig. 1. Colour composite MSX images of four regions. The Band A emission centred at 8.3 μ m, dominated by the UIBs, appears in turquoise. The Band E emission centred at 21.3 μ m, dominated by the continuum emission of small grains, appears in red. North is up and east is left. The field size is $20' \times 20'$ for Sh 104, $30' \times 30'$ for RCW 79, $18.3' \times 18.3'$ for RCW 82, and $23.3' \times 23.3'$ for RCW 120.

assume that any cluster containing a star massive enough to form an H II region (at least a B2V star) should be more luminous than $\sim 10000\,L_\odot$. The far-IR luminosities confirm that the sources detected at the border of Sh 212, Sh 259, RCW 34 and Dutra 45 most probably contain stars massive enough to ionize the gas. This is also probably the case for the sources associated with Sh 241 and Dutra 46. The results are contradictory

for RCW 40 (12) and RCW 82 (18): either they do not have the colours of UC H π regions or they are not luminous enough. And finally, both the MSX colours and the far-IR luminosities indicate that the point sources associated with RCW 82 (17) and RCW 120 do not contain massive stars.

Table 2. IR luminosities and colours of the selected sources.

	MSX point source						IRAS point source					
		F_8	F_{12}	F_{14}	F_{21}		F_{12}	F_{25}	F_{60}	F_{100}	$L_{ m FIR}$	
		(Jy)	(Jy)	(Jy)	(Jy)		(Jy)	(Jy)	(Jy)	(Jy)	(L_{\odot})	
1	Sh 104	8.39	10.45	7.36	41.54	20160 + 3636	15.2	94.2	647	1160	30000	
2	X	2.99	4.10	1.88	2.85							
3	Y	0.65	0.93			00580 + 6238	1.91	1.76	28.5	108	400	
4	Sh 212	2.27	2.91	4.94	35.34	04366 + 5022	2.87	54.2	199	470	35000	
5	Sh 217					04547 + 4753	10.4	82.0	36.0	367	13000	
6	Sh 219	1.60	2.11	2.01	3.00	04523 + 4718	3.30	5.21	81.7	305	8000	
7	Z	2.08	2.66	1.35	3.58	05197 + 3355	6.84	15.6	270	581	2500-8000	
8	Sh 241					06006 + 3015	1.94	11.8	189	552	14000	
9	Sh 259	1.00	2.05	3.25	13.85	06084 + 1727	3.22	24.8	124	263	28000	
10	RCW 34	7.47	17.37	20.64	75.97	08546 - 4254	2.93	194	1340	2100	34000	
11	RCW 40	3.23	5.50	2.53	5.69							
12	RCW 40	2.62	3.21	1.09	2.43	09007 - 4827	16.0	19.4	995	2620	17000	
13	Dutra 45	6.84	16.96	36.49	197.2	10184 - 5748	31.8	349	3330	5410	178000	
14	Dutra 46	2.71	5.49	4.62	10.33	10276 - 5711	12.5	61.4	492	1250	62000	
15	RCW 71	2.28	4.77	2.10	4.36	12474 - 6119	8.39	30.0	548	1420	7500	
16	RCW 79	3.64	10.04	13.33	33.10	13374 - 6130	25.1	95.5	1020	2850	55000	
17	RCW 82	1.34	1.98	1.99	5.99	13563 - 6109	2.76	12.60	104	319	3000	
18	RCW 82	0.64	2.44	5.48	6.88	13555 - 6107	7.0	14.7	136	576	5000	
19	RCW 120	2.76	3.42	2.08	2.92	17092 - 3823	4.66	8.43	73.1	3920	4000	

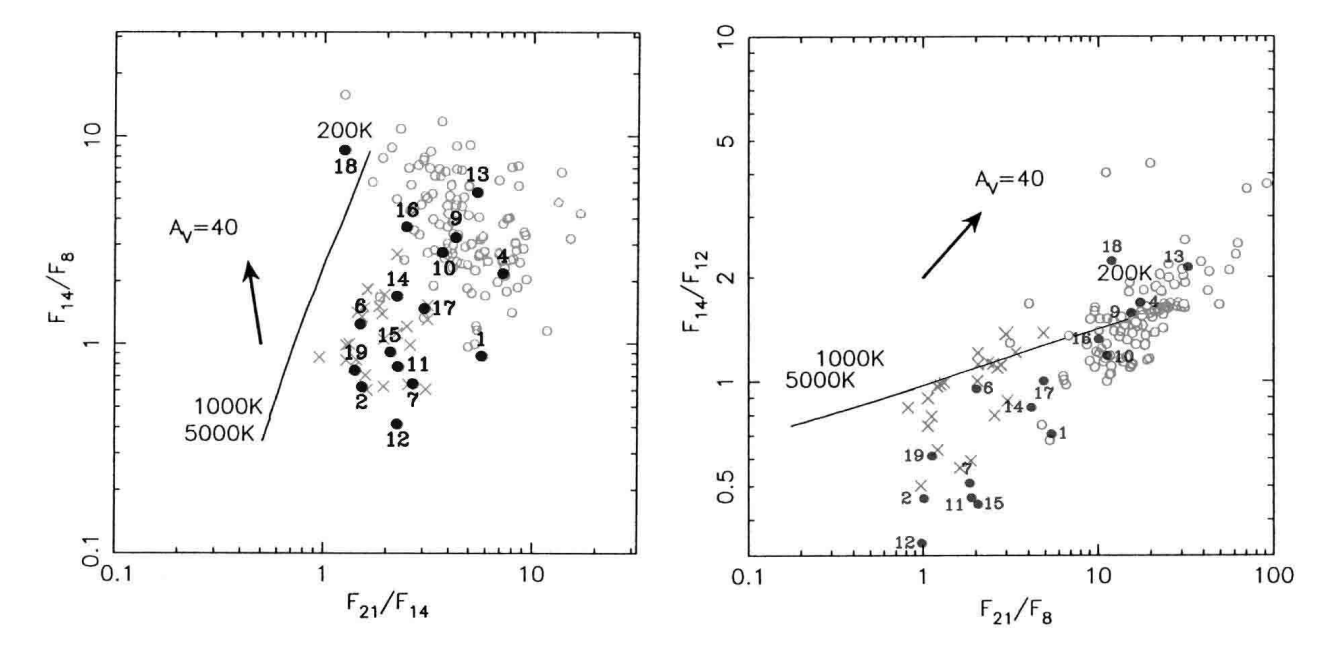


Fig. 2. Mid-IR colour-colour plots of the MSX point sources (black filled circles); the sources are identified by their numbers in Tables 1 and 2. The underlying figure is from Lumsden et al. (2002), with their original symbols changed to grey; the grey crosses are Herbig Ae/Be stars, and the empty grey circles are UC H π regions. (Other objects in the original figure but not discussed here have been removed.)

5. Comments on individual sources

Figs 3 to 19 present, for almost all the regions of Table 1, the MSX Band A emission, as contours superimposed on an optical image of the H II region (extracted from the DSS-2red survey or from the SuperCOSMOS H-alpha survey, Parker & Phillipps 1998). Exceptions are source X and Dutra 45, with no optically visible central H II region; in these cases we have used the radio

continuum emission to locate the ionized gas. A few comments are given for each source, mainly about the morphologies of the various components of the complexes.

5.1. Northern hemisphere regions

Sh 104 (Deharveng et al. 2003b) is the prototype of the sort of $H \, \text{II}$ region we are looking for in order to illustrate and test the

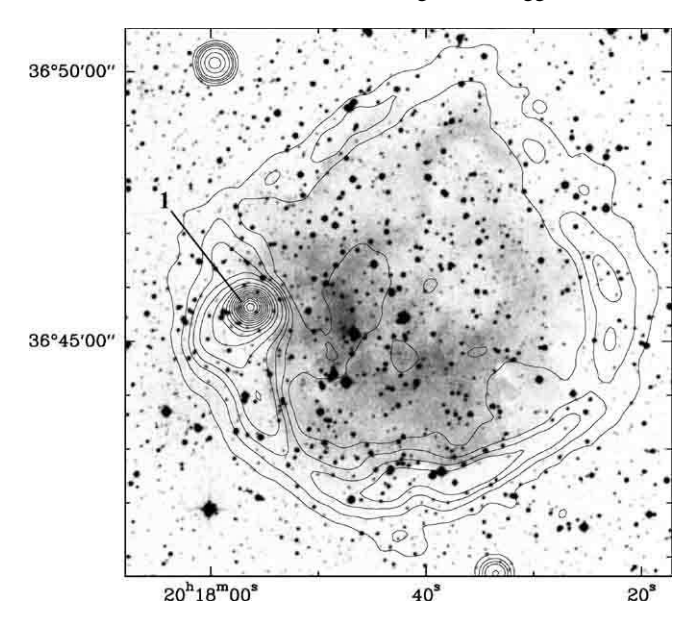


Fig. 3. Sh 104. MSX Band A emission (contours) superimposed on a DSS-2 red image. The first contour levels are at 3×10^{-6} and 4×10^{-6} , and then increase in steps of 4×10^{-6} W m⁻² sr⁻¹.

collect and collapse model. Sh 104 is a 7' diameter optically visible H $\scriptstyle\rm II$ region, excited by an O6V central star. This region is spectacular in the MSX Band A survey (Fig. 1), where a complete ring of dust emission surrounds the ionized gas. An MSX point source lies exactly on the dust ring. Near-IR observations show that this source harbours a deeply embedded cluster which, since it is associated with a UC H $\scriptstyle\rm II$ region, must contain at least one massive OB2 star. Our IRAM observations show that a ring of molecular material surrounds Sh 104. This ring contains four dense fragments *regularly spaced along the ring* and each formed of several dense cores. The cluster is embedded within the brightest fragment, whose mass is \sim 670 M_{\odot} .

Source X The central H π region is not optically visible, but is a radio continuum source of flux density 37.3 mJy at 1.4 GHz (NVSS Survey). Its distance is unknown. MSX Band A emission surrounds this H π region on its north, east and south sides. The brightness of the ring is clearly enhanced in the north-east; a cluster of near-IR objects lies in this direction. Another bright and very red MSX point source, observed 3'.2 north of the ring, corresponds to Mol 121 (Molinari et al. 1998), a UC H π region containing a small cluster of near-IR objects (as shown by our CFHT JHK images).

Source Y is a faint unnamed optical nebulosity of diameter $\sim 1.'0$. It corresponds to a very faint radio continuum source of flux density 3.5 mJy at 1.4 GHz (NVSS Survey). The distance of this region is 1.9 kpc (Kerton 2002). A half-ring of MSX Band A emission is observed exterior to the H II region. This emission is enhanced just north of the source, and several bright near-IR stars are observed in this direction (but no emission is detected at 14 μm and 21 μm). A molecular cloud, of 185 M_{\odot} , also lies just north of source Y (Kerton 2002).

Sh 212 is a bright optical H π region, of diameter $\sim 5'$, nearly circular around its central exciting cluster. It is a high excitation region, ionized mainly by an O5.5neb star, at a dis-

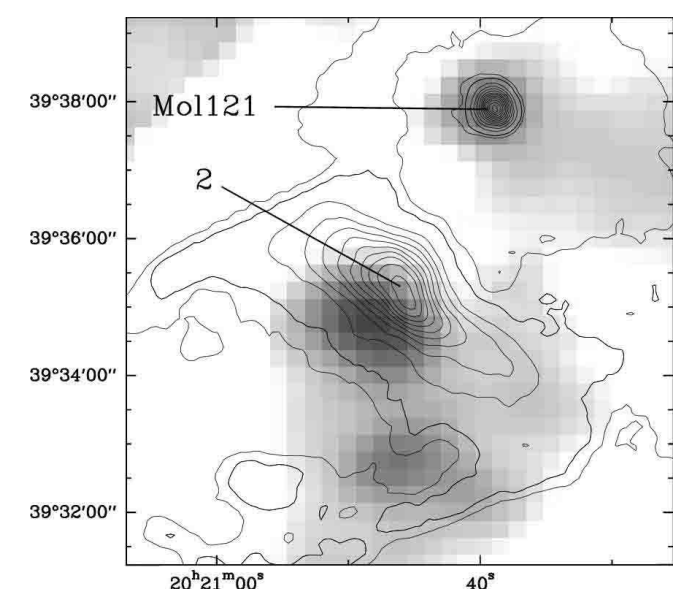


Fig. 4. Source X. MSX Band A contours superimposed on a 1.4 GHz continuum. The first contour levels are at 4×10^{-6} and 5×10^{-6} , and then increase in steps of 3×10^{-6} W m⁻² sr⁻¹.

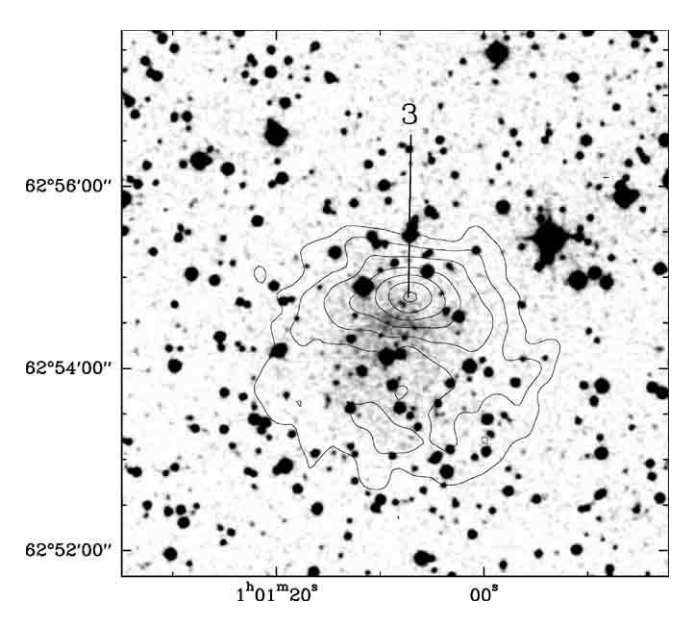


Fig. 5. Source Y. MSX Band A contours superimposed on a DSS-2 red image. The first contour levels are at 1.4×10^{-6} and 2×10^{-6} , and then increase in steps of 1×10^{-6} W m⁻² sr⁻¹.

tance of 7.1 kpc (Caplan et al. 2000). A ring of MSX emission surrounds the bright northern part of the H II region (but not all of it). A bright MSX point source lies along this ring, north-west of Sh 212. An optical reflection nebula and a bright near-IR source are observed in this direction.

Sh 217 is an elliptical optical H $\scriptstyle\rm II$ region, $10' \times 7'.5$ in size, excited by a central O9V star. Its distance is 5.0 kpc. There is a half-ring of MSX Band A emission south and west of this H $\scriptstyle\rm II$ region. A bright MSX point source is observed in the middle of the arc. This corresponds to a deeply embedded near-IR cluster which contains at least one OB2 star, as it is associated with a UC H $\scriptstyle\rm II$ region (Deharveng et al. 2003a). Molecular condensa-

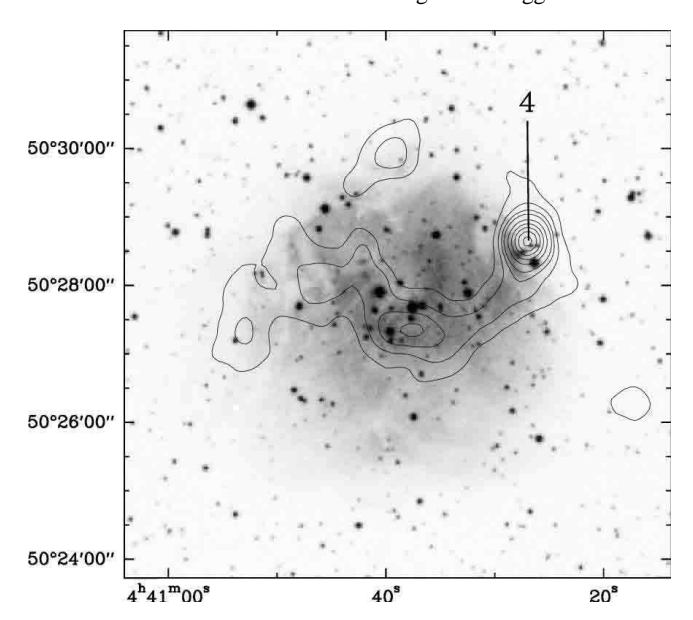


Fig. 6. Sh 212. MSX Band A contours superimposed on a DSS-2 red image. The first contour levels are at 2×10^{-6} , 3×10^{-6} , 4×10^{-6} and 5×10^{-6} , and then increase in steps of 2×10^{-6} W m⁻² sr⁻¹.

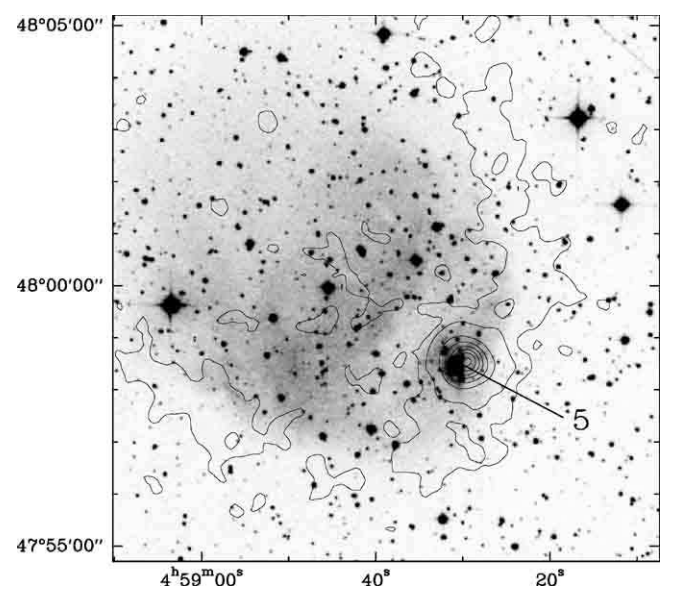


Fig. 7. Sh 217. MSX Band A contours superimposed on a DSS-2 red image. The first contour levels are at 1×10^{-6} and 2×10^{-6} , and then increase in steps of 5×10^{-6} W m⁻² sr⁻¹.

tions are present south and west of this H II region; the brightest one lies in the direction of the cluster (Brand et al. in preparation). Half a ring of low density atomic hydrogen curves around the ionized gas to the north and east (Roger & Leahy 1993).

Sh 219 is a spherical H II region, of diameter 1.5, excited by a B0V star. Its distance is 5.0 kpc. Half a ring of MSX dust emission encloses the H II region on its south and west sides. This ring is enhanced in the middle of the arc, where a deeply embedded cluster is observed elongated along the ring (Deharveng et al. 2003a). An H α emission star with a near-IR excess, and affected by a visual extinction \sim 24 mag, lies near

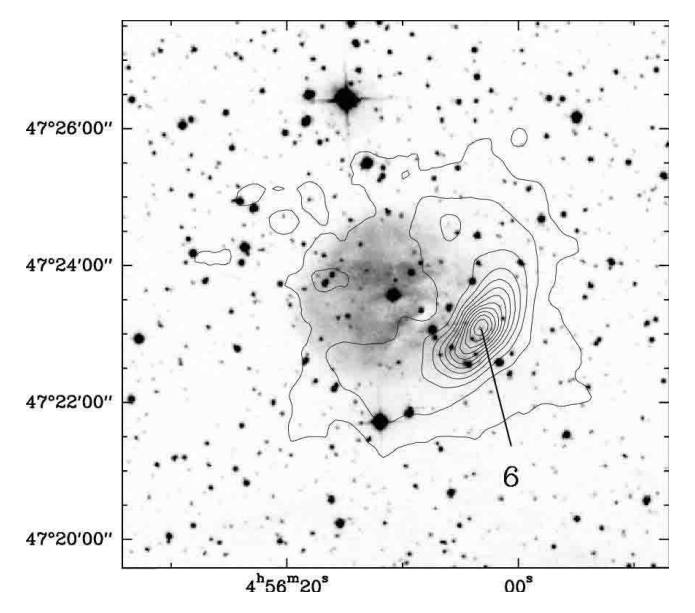


Fig. 8. Sh 219. MSX Band A contours superimposed on a DSS-2 red image. The contour levels begin at 1×10^{-6} and increase in steps of 1×10^{-6} W m⁻² sr⁻¹.

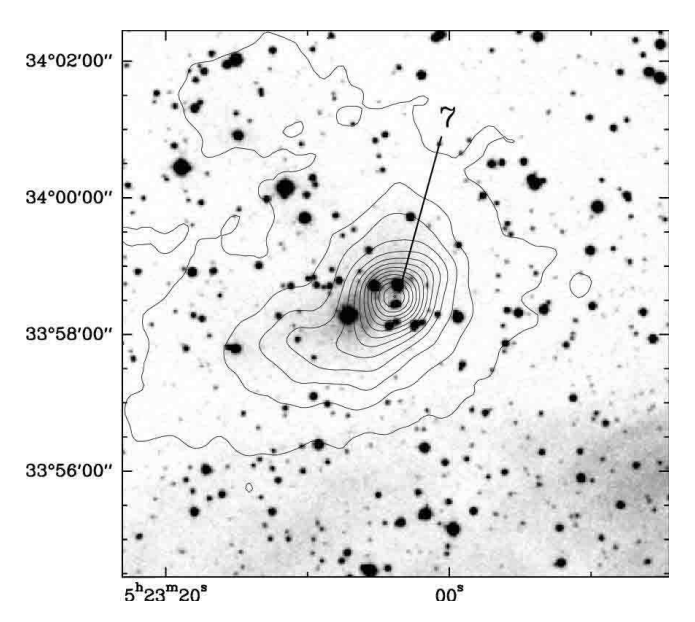


Fig. 9. Source Z. MSX Band A contours superimposed on a DSS-2 red image. The contour levels begin at 1×10^{-6} and increase in steps of 1.5×10^{-6} W m⁻² sr⁻¹.

the centre of the cluster. The presence nearby of a UC H π region (Leahy 1997) remains to be confirmed. A molecular condensation is observed in the direction of the cluster (Lefloch et al. in preparation). Elsewhere the ionized gas is surrounded by a low density atomic hydrogen ring (Roger & Leahy 1993).

Source Z is a small unnamed optical nebulosity, of diameter ~ 1.5 , located at the edge of the large diffuse H II region Sh 230. It is also a faint radio continuum source (Carpenter et al. 1990 and NVSS survey). The distance of this region is very uncertain: 1.8 kpc is its kinematic distance (Wouterloot & Brand 1989) and 3.2 kpc is the photometric distance of the nearby H II regions (with similar velocities) Sh 236 and Sh 237

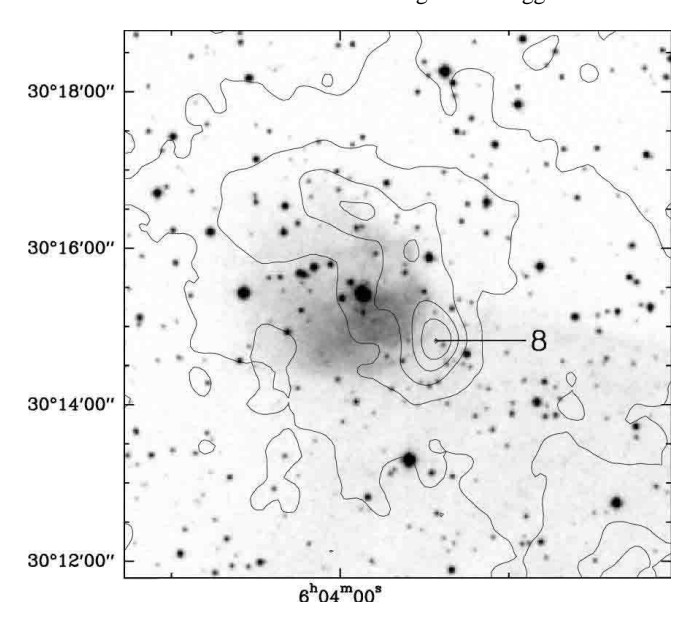


Fig. 10. Sh 241. MSX Band A contours superimposed on a DSS-2 red image. The contour levels begin at 1×10^{-6} and increase in steps of 1.5×10^{-6} W m⁻² sr⁻¹.

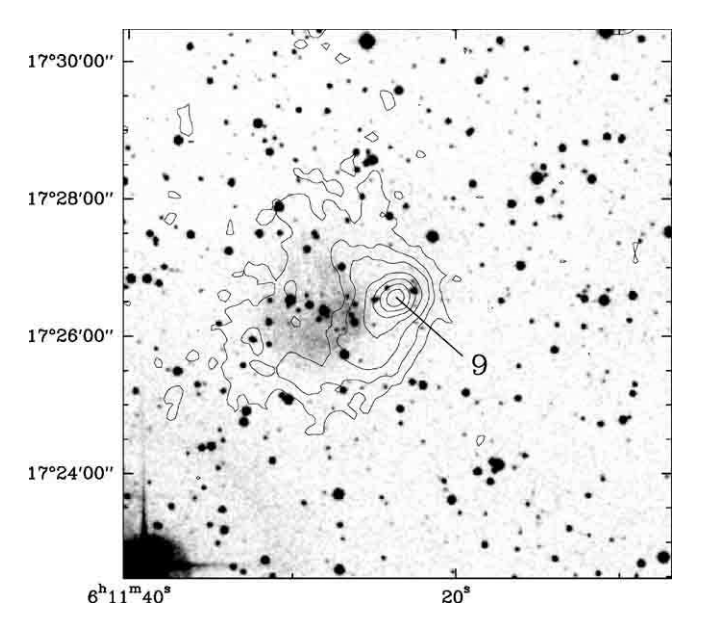
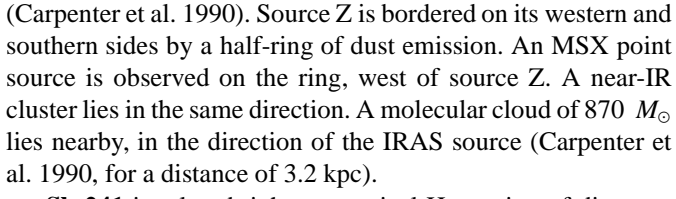


Fig. 11. Sh 259. MSX Band A contours superimposed on a DSS-2 red image. The contour levels begin at 1.5×10^{-6} and increase in steps of 1.5×10^{-6} W m⁻² sr⁻¹.



Sh 241 is a low-brightness optical H π region of diameter 10'. A brighter (but unnamed), nearly spherical H π region of diameter $\sim 2'$ lies at its north-east corner. We are interested in this brighter region, excited by a central O9V star, and lying at a distance of 4.7 kpc (Moffat et al. 1979). Half a ring of dust emission borders this brighter H π region to the north

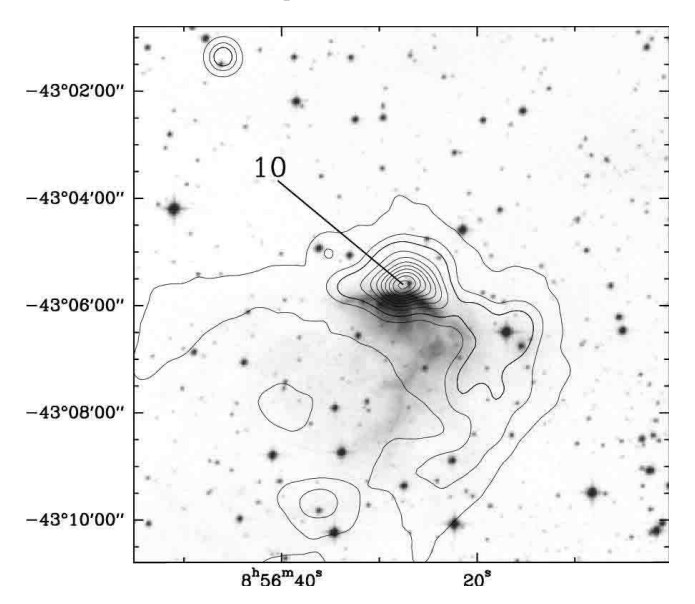


Fig. 12. RCW 34. MSX Band A contours superimposed on a DSS-2 red image. The first contour levels are at 3×10^{-6} , 6×10^{-6} and 9×10^{-6} , and then increase in steps of 6×10^{-6} W m⁻² sr⁻¹.

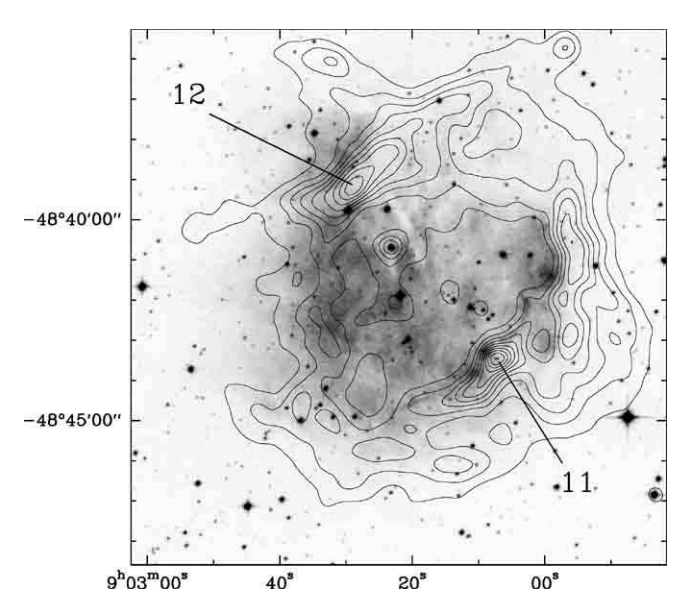


Fig. 13. RCW 40. MSX Band A contours superimposed on a DSS-2 red image. The contour levels begin at 5×10^{-6} and increase in steps of 3×10^{-6} W m⁻² sr⁻¹.

and east. An MSX point source lies at the southern extremity of the arc (which is not listed in the MSX Point Source Catalog), and a near-IR cluster is also observed in this direction. Nearby is a dense molecular core which has been observed in the CS and HCN lines (Plume et al. 1992, 1997, Pirogov 1999), and mapped at 350 μ m (Mueller et al. 2002). An H₂O maser (Cesaroni et al. 1988, Henning et al. 1992) and a molecular outflow (Wu et al. 1999) have also been detected in the direction of the MSX and IRAS point sources, demonstrating that massive-star formation is presently taking place.

Sh 259 is a low-brightness optical H $\scriptstyle\rm II$ region, of diameter \sim 2'. It lies in the general direction of the Gemini OB1 molecular

complex, but is most probably a foreground object (Carpenter et al. 1995). Sh 259 is nearly circular around a central B1 star, and lies at 8.3 kpc (Moffat et al. 1979). It is a thermal radio continuum source (Wouterloot et al. 1988, Fich 1993) and is bordered to the west by a half-ring of MSX emission. An MSX point source lies in the middle of the arc. Near-IR objects are observed in this direction. However, no H₂O maser has been detected (Wouterloot et al. 1993).

5.2. Southern hemisphere regions

RCW 34 is a cometary shaped H II region, located at 3.1 kpc and excited by an O9Ib star (Russeil et al. 2003, Avedisova & Kondratenko 1984). MSX Band A emission surrounds the ionized region with a bright MSX and IRAS point source located just in front of the bright ionization front. Near-IR observations indicate that star formation is observed at the border of the ionization front (Zavagno et al. in preparation).

RCW 40 is an 8′ diameter H π region located at 1.84 kpc and excited by an O9V star (Avedisova & Kondratenko 1984). It is surrounded by a complete ring of dust emission, with bright MSX and IRAS point sources observed along the ring. The 1.2-mm continuum observations reveal the presence of several bright condensations along the ring (Zavagno et al. in preparation). This indicates that the collect and collapse process may be at work here.

Dutra 45 - Gal 284.0-0.9 is located at 4.5 kpc (Russeil 2003). An IR cluster (no. 45 in Dutra et al. 2003) lies at the western edge of a faint optical nebulosity (Fig. 14 *Right*). A large-field image of this region (Fig. 14 *Left*) reveals the presence of a dust ring surrounding a radio emission region of 15' diameter (Condon et al. 1993, observations at 4850 MHz). The near-IR cluster that corresponds to the bright MSX point source listed in Table 1 has been observed in the near IR. The images reveal the presence of a filamentary structure that follows the optical ionization front (Zavagno et al. in preparation). This filament contains numerous bright and very red objects, indicating that star formation is taking place there.

Dutra 46 - Gal 284.723+0.313 lies at a distance of 6.2 kpc (Bronfman et al. 1996). Faint optical emission is observed, surrounded by extended MSX Band A emission. Our near-IR observations of the MSX point source reveal the presence of two very bright, red clusters. The brighter one corresponds to no. 46 in Dutra et al. (2003). Star formation is ongoing at the border of the ionized structure.

RCW 71 is located at 2.1 kpc and is excited by an O9.5V star (Russeil 2003, Avedisova & Kondratenko 1984). The ionized region is surrounded by a complete ring of MSX Band A emission. A bright MSX point source is observed on the ring, south-east of the H II region. The 1.2-mm continuum observations reveal the presence of five condensations along the dust ring (Zavagno et al. in preparation), indicating that star formation is taking place there, possibly by the collect and collapse mechanism.

RCW 79 is a bright optical H $\scriptstyle\rm II$ region of diameter $\sim 10'$, located at 4.2 kpc (Russeil 2003). It is excited by a central 08V star and has been studied in detail by Cohen et al. (2002). This

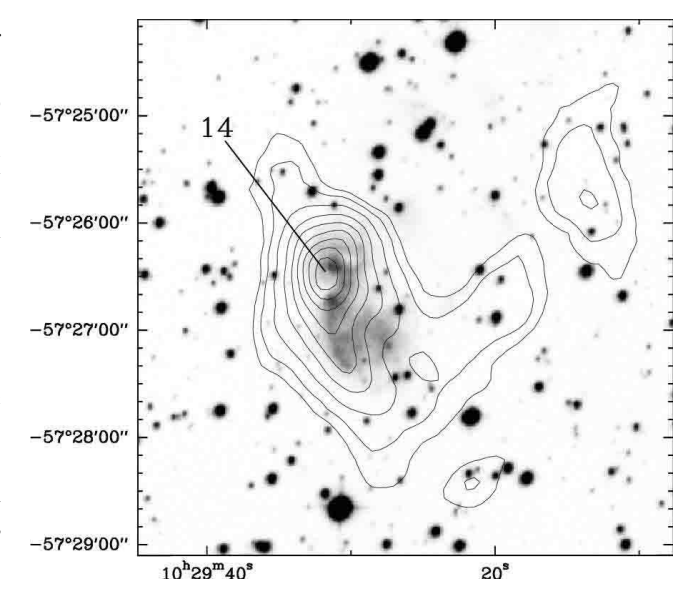


Fig. 15. Dutra 46. MSX Band A contours superimposed on an H α image from SuperCOSMOS. The first contour levels are at 5×10^{-6} and 7×10^{-6} and then increase in steps of 3×10^{-6} W m⁻² sr⁻¹.

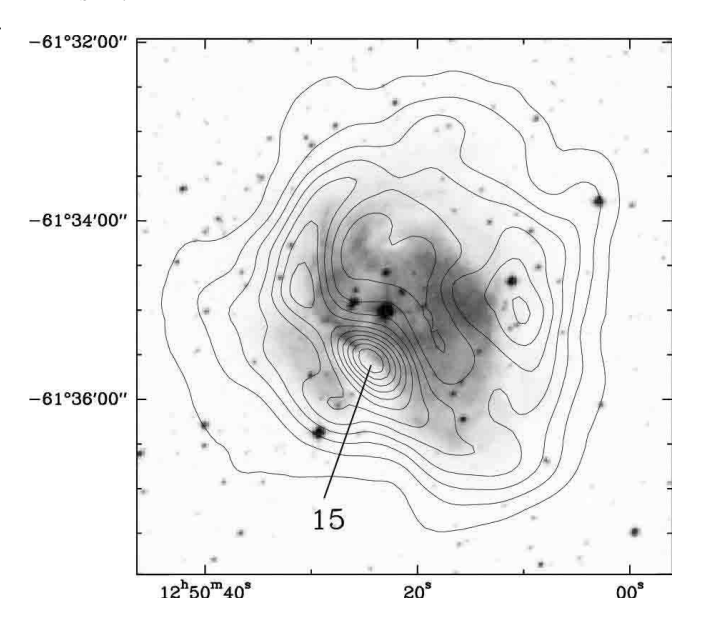


Fig. 16. RCW 71. MSX Band A contours superimposed on a DSS-2 red image. The contour levels begin at 4×10^{-6} and increase in steps of 2×10^{-6} W m⁻² sr⁻¹.

region is surrounded by MSX Band A emission (Fig. 1). The MSX point source listed in Table 1 is double-peaked. A compact H II region (Cohen et al. 2002) coincides with the brightest peak. Our near-IR observations reveal the presence of a bright cluster containing OB stars (Zavagno et al. in preparation). The other peak is fainter, redder, and is associated with maser emission (Caswell 2004) suggesting that ongoing massive-star formation is taking place. Moreover, our 1.2-mm continuum emission observations reveal the presence of massive fragments distributed along the dust ring (Zavagno et al. in preparation). These data strongly suggest that the collect and collapse process is at work in this region.

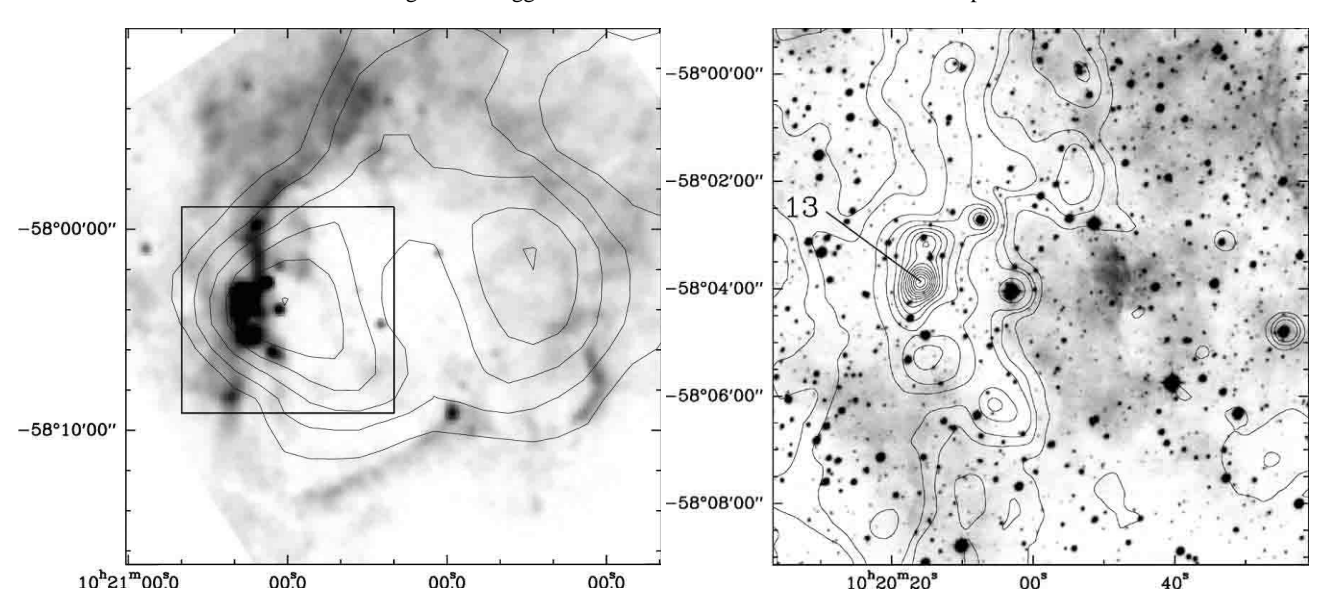


Fig. 14. Dutra 45. *Left:* radio continuum emission at 4850 MHz (contours) superimposed on an MSX Band A image; the square represents the field of the right image. *Right:* MSX Band A contours superimposed on an H α image from SuperCOSMOS. The contour levels begin at 4×10^{-6} and increase in steps of 3×10^{-6} W m⁻² sr⁻¹.

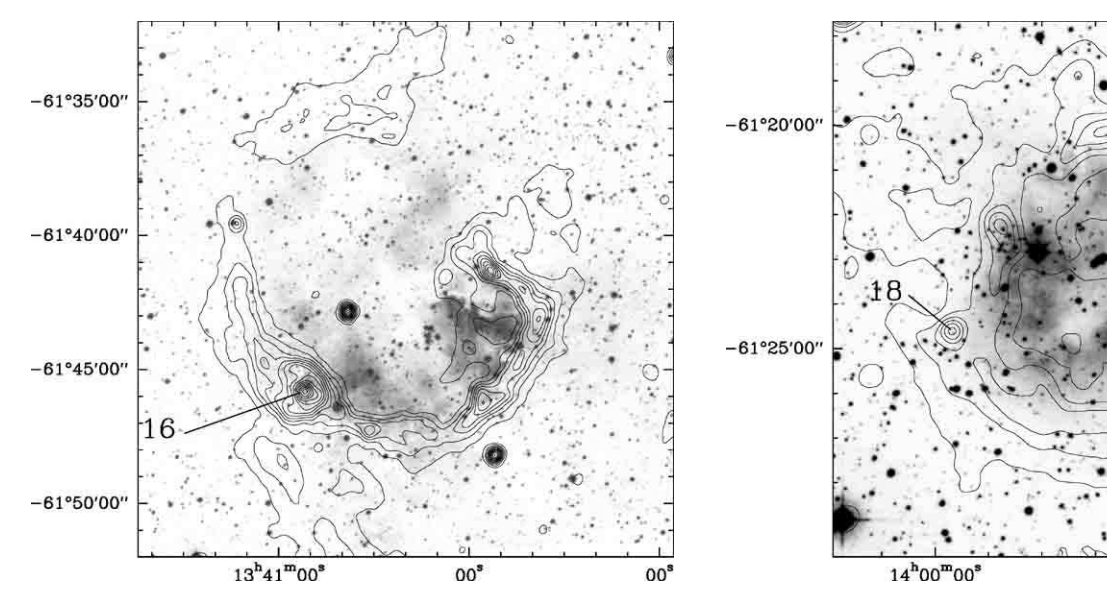


Fig. 17. RCW 79. MSX Band A contours superimposed on an H α image from SuperCOSMOS. The contour levels begin at 5×10^{-6} and increase in steps of 3×10^{-6} W m⁻² sr⁻¹.

Fig. 18. RCW 82. MSX Band A contours superimposed on an H α image from SuperCOSMOS. The contour levels begin at 3×10^{-6} and increase in steps of 2×10^{-6} W m⁻² sr⁻¹.

RCW 82 is located at 2.9 kpc (Russeil 2003), and has an optical diameter of $\sim 5'$. It is surrounded by a nearly complete MSX Band A emission ring (Fig. 1). Two bright MSX point sources are observed along this ring, diametrically opposite each other. Point source 17 (in Table 1) corresponds to near-IR sources which are bright and red (Zavagno et al. in preparation). Bright, red stars are also observed in the direction of the point source 18 (2MASS K_S survey). This indicates that star formation is taking place in the dust ring that surrounds RCW 82.

RCW 120 is located at 1.2 kpc and is excited by an O6V star (Russeil 2003, Avedisova & Kondratenko 1984). Its opti-

cal diameter is about 8'. This region is almost completely surrounded by a ring of MSX Band A emission (Fig. 1). Dust continuum emission at 1.2 mm reveals the presence of five fragments distributed along the ring (Zavagno et al. in preparation). One of them corresponds to the MSX point source listed in Table 1. The dust ring is well defined south of RCW 120, is elongated north-south, and is possibly open at its northern extremity. The ionized gas seems to flow away from the H $\scriptstyle\rm II$ region through this hole. A similar picture is given by RCW 79. These two H $\scriptstyle\rm II$ regions have possibly evolved in a medium having a density gradient, and are presently experiencing a champagne flow, after the fragmentation of their sur-

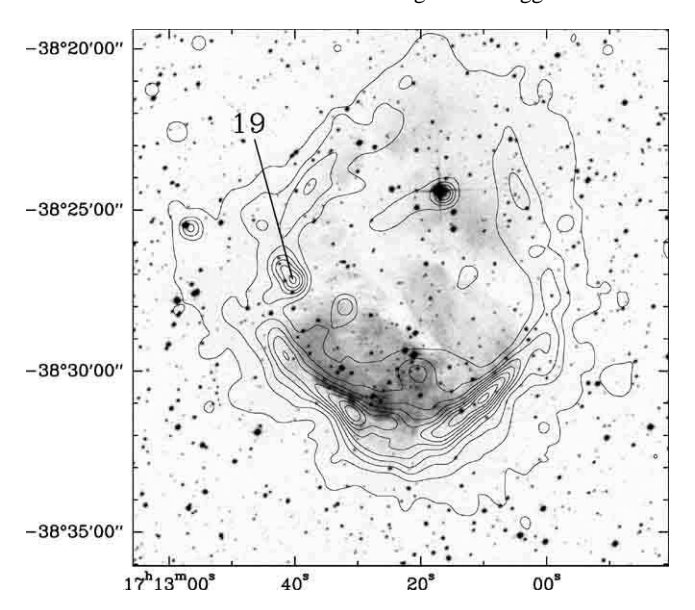


Fig. 19. RCW 120. MSX Band A contours superimposed on a DSS-2 red image. The contour levels begin at 4×10^{-6} and increase in steps of 3×10^{-6} W m⁻² sr⁻¹.

rounding dust rings. The presence of cold dust condensations on the ring, along with the presence of near-IR objects detected with 2MASS, indicates that the collect and collapse process may be at work here.

6. Discussion and conclusion

We have selected seventeen H II regions with a very simple morphology. These regions are relatively isolated, most of them being situated somewhat north or south of the Galactic plane. The survival of an annular structure around an ionized region may be easier in 'quiet' zones (our selection is deliberately biased toward regions presenting a simple morphology, and this is favoured by quiet surroundings).

We have observed most of these MSX point sources in the near IR, at the CFH or at the ESO NTT, in order to determine their stellar contents. The associated embedded clusters, when present, are possibly second-generation clusters. Some of them - those associated with Sh 104, Sh 217 and RCW 79 - contain massive stars exciting UC H II regions. We have shown that a few others - those associated with Sh 212, Sh 241, Sh 259, RCW 34, Dutra 45 and Dutra 46 – also probably contain massive stars; this last point remains to be confirmed. The structure of these clusters, if they are confirmed to be second-generation clusters - hence young relatively unevolved clusters - should give us information about the way massive stars form. Are the massive stars found in the very centres of the clusters, and do the clusters show mass segregation? In some regions, such as Sh 212, only a bright *isolated* source is observed. It seems very important, in the context of massive-star formation, to find similar isolated objects, and to estimate their masses and their evolutionary stages.

We have observed the molecular and dust environment of a few $H\pi$ regions at millimetre wavelengths. The molecular line emission in Sh 104, Sh 217 and Sh 219 was mapped at

IRAM. The continuum emission of cold dust, at 1.2 mm, was mapped with the SEST at ESO in RCW 40, RCW 71, RCW 79 and RCW 120, and with MAMBO at IRAM in Sh 217, source Z, Sh 241 and Sh 259. These observations are important because only the presence of a dense molecular shell surrounding the ionized gas, or the presence of massive fragments regularly spaced along the ionization front, can prove that we are dealing with the collect and collapse process. This is definitely the case for Sh 104 (Deharveng et al. 2003b), and most probably the case for RCW 79 (Zavagno et al. in preparation). The situation is unclear for Sh 217 and especially Sh 219, which are partially surrounded by a low density ring of atomic (and not high density molecular) hydrogen.

With our criteria we have selected two types of H $\scriptstyle\rm II$ regions. Some (Sh 104, RCW 40, RCW 79, RCW 82 and RCW 120) are surrounded by a nearly complete ring of dust emission. Some others are low brightness H $\scriptstyle\rm II$ regions, surrounded by an incomplete ring of dust emission (source Z, Sh 219, Sh 241 and Sh 259). Star formation is presently taking place at the periphery of Sh 241, as well as at the periphery of RCW 79, as attested by the detection of H₂O masers at the peripheries of both of these regions. It will be interesting to determine if the collect and collapse process is at work in both types of H $\scriptstyle\rm II$ regions, and if the same kind of stars are formed.

In a few cases one may wonder if the cluster observed at the periphery of the H II region is not the primary source of ionization of the gas, the extended H II region being a blister on the surface of the molecular cloud, with the ionized gas flowing away from the cloud. In the case of Sh 219 for example, there is some evidence for a 'Champagne flow': the velocity of the ionized gas is $\sim 6 \text{ km s}^{-1}$ more negative than that of the molecular material (Deharveng et al. 2003a). However, the exciting star of Sh 219 is clearly identified, and lies at the centre of the H_{II} region and not in the cluster observed at its periphery. The regions Sh 104, Sh 212, Sh 217, Sh 241, Sh 259, RCW 40, RCW 79 and RCW 120 are also excited by identified stars lying near their centres. Lopsided RCW 34 is possibly a blister H II region, but its exciting star is identified (Heydari-Malayeri 1988); it lies near the ionization front but is separated from the MSX point source. Nothing is known about the exciting stars of sources X, Y, Z and Dutra 46.

The molecular or cold dust condensations observed at the periphery of a given region contain objects in various evolutionary stages. For example, around RCW 79 are found: i) a near-IR cluster associated with a compact H $\scriptstyle\rm II$ region – thus already a bit evolved; ii) a red MSX point source, in the direction of which an H $_2$ O maser is detected – hence a present site of star formation; iii) condensations with no associated near- or mid-IR sources, thus, possibly, recently formed by fragmentation, or containing class 0 objects. This indicates either that the fragmentation of the compressed layer spreads over time, or that the fragments evolve at different rates – a complication compared to the models.

In several regions, such as Sh 104, RCW 79 and RCW 120, the molecular or cold dust condensations are almost all observed in the direction of the dust ring, as if the fragmentation (and subsequent star formation) were taking place in a preferential plane perpendicular to the line of sight. This is not pre-

dicted by the collect and collapse model, where fragmentation occurs in the spherical shell, at the periphery of the ionized region (so a few condensations should be observed inside the ring). A new model which can explain these observations is presently being developed by A. Whitworth (private communication).

Acknowledgements. We would like to thank R. Cautain for his development of procedures to transform the images, and Y. Brand, B. Lefloch and F. Massi for their collaboration in this long term project. This research has made use of the Simbad astronomical database operated at CDS, Strasbourg, France, and of the interactive sky atlas Aladin (Bonnarel et al. 2000). This publication uses data products from the Midcourse Space EXperiment, from the Two Micron All Sky Survey and from the InfraRed Astronomical Satellite; for these we have used the NASA/IPAC Infrared Science Archive, which is operated by the Jet Propulsion Laboratory, California Institute of Technology, under contract with the National Aeronautics and Space Administration. We have also used the SuperCOSMOS, NVSS and GB6 surveys.

References

Avedisova, V.S., Kondratenko, G.I. 1984, Nauchnye Informatsii, 56, 59

Bertoldi, F. 1989, ApJ, 346, 735

Bertoldi, F., McKee, C. 1990, ApJ, 354, 529

Bonnarel, F., Fernique, P., Bienayme, O., Egret, D., Genova, F., Louys, M., Ochsenbein, F., Wenger, M., Bartlett, J.G. 2000, A&ASS, 143, 33

Bouwman, J., Meeus, G., de Koter, A., Hony, S., Dominik, C., Waters, L.B.F.M. 2001, A&A, 375, 950

Bronfman, L., Nyman, L.-A., May, J. 1996, A&AS, 115, 81

Caplan, J., Deharveng, L., Peña, M., Costero, R., Blondel, C. 2000, MNRAS, 311, 317

Carpenter, J.M., Snell, R.L., Schloerb, F.P. 1990, ApJ, 362, 147

Carpenter, J.M., Snell, R.L., Schloerb, F.P. 1995, ApJ, 445, 246

Caswell, J.L. 2004, MNRAS, 351, 279

Cesaroni, R., Palagi, F., Felli, M., Catarzi, M., Comoretto, G., Di Francos, S., Giovanardi, C., Palla, F. 1988, A&AS, 76, 445

Cesarsky, D., Jones, A.P., Lequeux, J., Verstraete, L. 2000, A&A, 358, 708

Cohen, M., Green, A.J., Parker, Q.A., Mader, S., Cannon, R.D. 2002, MNRAS, 336, 736

Condon, J.J., Griffith, M.R., Wright, A.E. 1993, AJ, 106, 1095

Condon, J.J., Cotton, W.D., Greisen, E.W., Yin, Q.F., Perley, R.A., Taylor, G.B., Broderick, J.J. 1998, AJ, 115, 1693

Conti, P.S., Crowther P.A. 2003, preprint (astro-ph/0307365)

Crowther P.A., Conti, P.S. 2003, MNRAS, 343, 143

Crété, E., Giard, M., Joblin, C., Vauglin, I., Léger, A., Rouan, D. 1999, A&A, 352, 277

Deharveng, L., Zavagno, A., Salas, L., Porras, A., Caplan, J., Cruz-González, I. 2003a, A&A, 399, 1135

Deharveng, L., Lefloch, B., Zavagno, A., Caplan, J., Whitworth, A.P., Nadeau, D., Martin, S. 2003, A&A, 408, L25

Dobashi, K., Yonekura, Y., Matsumoto, T., Momose, M., Sato, F., Bernard, J-P., Ogawa, H. 2001, PASJ, 53, 85

Dutra, C.M., Bica, E., Soares, J., Barbuy, B. 2003, A&A, 400, 533

Dyson, J.E., Williams, D.A. 1997, The physics of the interstellar medium, 2nd ed., eds R J Tayler & M Elvis, Published by Institute of Physics Publishing, Bristol and Philadelphia

Egan, M.P., Price, S.D., Moshir, M.M., et al. 1999, The Midcourse Space Experiment Point Source Catalog Version 1.2, Explanatory Guide, AFRL-VS-TR-1999-1522, Air Force Research Laboratory Egan, M.P., Van Dyk, S.D., Price, S.P. 2001, AJ 122, 1844

Egan, M.P., Price, S.D., Kraemer, K.E., Mizuno, D.R., Carey, S.J., Wright, C.O., Engelke, C.W., Cohen, M., Gugliotti, M.G. 2003, AFRL-VS-TR-2003-1589, Air Force Research Laboratory

Elmegreen, B.G., Lada, C.J. 1977, ApJ 214, 725

Elmegreen, B.G., Kimura, T., Tosa, M. 1995, ApJ 451, 675

Elmegreen, B.G. 1998, in ASP Conf. Ser., 148, 150, eds. C.E. Woodward, J.M. Shull & H.A. Tronson

Emerson, J.P. 1988, in Dupree A.K., Lago M.T.V.T., eds, NATO ASI Ser. C, Vol 241, Formation and Evolution of Low Mass Stars. Kluwer, Dordrecht, p. 193

Faison, M., Churchwell, E., Hofner, P., Hackwell, J., Lynch, D.K., Russell, R.W. 1998, ApJ, 500, 280

Fich, M. 1993, ApJS 86, 475

Fukuda, N., Hanawa, T. 2000, ApJ, 533, 911

García-Segura, G., Franco, J. 1996, ApJ, 469, 171

Ghosh, S.K., Ojha, D.K. 2002, A&A, 388, 326

Henning, T., Cesaroni, R., Walmsley, M., Pfau, W. 1992, A&AS, 93, 525

Heydari-Malayeri, M. 1988, A&A, 202, 240

Karr, J.L., Martin, P.G. 2003, ApJ, 595, 900

Kerton, C.R. 2002, AJ, 124, 3449

Leahy, D.A. 1997, JRASC, 91, 127

Lefloch, B., Lazareff, B. 1994, A&A, 289, 559

Lefloch, B., Lazareff, B., Castets, A. 1997, A&A 324, 249

Léger, A., Puget, J.-L. 1984, A&A, 137, L5

Lumsden, S.L., Hoare, M.G., Oudmaijer, R.D., Richards, D. 2002, MNRAS, 336, 621

Meeus, G., Waters, L.B.F., Bouwman, M.E., van den Ancker, M.E., Waelkens, C., Malfait, K. 2001, A&A, 365, 476

Moffat, A.F.J., Ftzgerald, M.P., Jackson, P.D. 1979, A&AS, 38, 197
 Molinari, S., Brand, J., Cesaroni, R., Palla, F., Palumbo, G.G.C. 1998,
 A&A, 336, 339

Mueller, K.E., Shirley, Y.L., Evans II, N.J., Jacobson, H.R. 2002, ApJS, 143, 469

Ogura, K., Sugitani, K., Pickles, A. 2002, AJ, 123, 2597

Parker, Q.A., Phillipps, S. 1998, PASA, 15, 28

Peeters, E., Martín-Harnández, N.L., Damour, F., Cox, P., Roelfsema,
P.R., Baluteau, J.-P., Tielens, A.G.G.M, Churchwell, E., Kessler,
M., Mathis, J.S., Morisset, C., Schaerer, D. 2002, A&A, 381, 571
Pirogov, L. 1999, A&A, 348, 600

Plume, R., Jaffe, D.T., Evans II, N.J. 1992, ApJS, 78, 505

Plume, R., Jaffe, D.T., Evans II, N.J., Martín-Pintado, J., Gómez-González, J. 1997, ApJ, 476, 730

Price, S.D., Egan, S.M., Carey, S.J., Mizuno, D.R., Kuchar, T.A. 2001, AJ, 121, 2819

Roger, R.S., Leahy, D.A. 1993, AJ, 106, 31

Russeil, D. 2003, A&A, 397, 133

Smith, L., Norris, R.P.F., Crowther, P.A. 2002, MNRAS, 337, 1309

Sugitani, K., Fukui, Y., Mizuno, A., Ohashi, N. 1989, ApJ, 342, L87

Thompson, M.A., White G.J., Morgan, L.K., Miao, J., Friedlund, C.W.M., Huldtgren-White, M. 2004, A&A, 414, 1017

Whitworth, A.P., Bhattal, A.S., Chapman, S.J., Disney, M.J., Turner, J.A. 1994, MNRAS, 268, 291

Wouterloot, J.G.A., Brand, J., Henkel, C. 1988, A&A, 191, 323

Wouterloot, J.G.A., Brand, J. 1989, A&AS, 80, 149

Wouterloot, J.G.A., Brand, J., Fiegle, K. 1993, A&ASS, 98, 589

Wu, Y.-F., Yang, C.-Y., Li, Y.-X. 1999, Chinese Astron., 23, 6

Yamaguchi, N., Mizuno, N., Matsunaga, K., Mizuno, A., Ogawa, H., Fukui, Y. 1999, PASJ, 51, 775

Zavagno, A., Ducci, V. 2001, A&A, 371, 312